

*School of Natural Sciences and Mathematics
William B. Hanson Center for Space Sciences*

***Daytime Zonal Drifts in the Ionospheric 150km
and E Regions Estimated Using Ear Observations***

UT Dallas Author(s):

Russell A. Stoneback
R. A. Heelis

Rights:

©2017 American Geophysical Union

Citation:

Pavan Chaitanya, P., A. K. Patra, Y. Otsuka, T. Yokoyama, et al. 2017.
"Daytime zonal drifts in the ionospheric 150km and E regions estimated
using EAR observations." *Journal of Geophysical Research--Space Physics*
122(8), doi:10.1002/2017JA024589

*This document is being made freely available by the Eugene McDermott Library
of the University of Texas at Dallas with permission of the copyright owner. All
rights are reserved under United States copyright law unless specified otherwise.*

RESEARCH ARTICLE

10.1002/2017JA024589

Key Points:

- Provide first radar measurements of daytime zonal plasma drifts at the 150 km and *E* regions over Indonesia
- The 150 km and *E* region zonal drifts are westward and are comparable
- Zonal drifts at the 150 km region are less than the C/NOFS measured *F* region drifts indicating vertical shear in the zonal drift

Correspondence to:

A. K. Patra,
akpatra@narl.gov.in

Citation:

Pavan Chaitanya, P., A. K. Patra, Y. Otsuka, T. Yokoyama, M. Yamamoto, R. A. Stoneback, and R. A. Heelis (2017), Daytime zonal drifts in the ionospheric 150 km and *E* regions estimated using EAR observations, *J. Geophys. Res. Space Physics*, 122, 9045–9055, doi:10.1002/2017JA024589.


Received 13 JUL 2017

Accepted 11 AUG 2017

Accepted article online 16 AUG 2017

Published online 31 AUG 2017

Daytime zonal drifts in the ionospheric 150 km and *E* regions estimated using EAR observations

P. Pavan Chaitanya¹, A. K. Patra¹ , Y. Otsuka² , T. Yokoyama³ , M. Yamamoto⁴ , R. A. Stoneback⁵ , and R. A. Heelis⁵ 
¹National Atmospheric Research Laboratory, Gadanki, India, ²Institute for Space-Earth Environmental Research, Nagoya University, Nagoya, Japan, ³National Institute of Information and Communications Technology, Tokyo, Japan, ⁴Research Institute for Sustainable Humanosphere, Kyoto University, Kyoto, Japan, ⁵Hanson Center for Space Sciences, Physics Department, University of Texas at Dallas, Richardson, Texas, USA

Abstract Multibeam observations of the 150 km echoes made using the Equatorial Atmosphere Radar (EAR), located at Kototabang, Indonesia, provide unique opportunity to study both vertical and zonal $\mathbf{E} \times \mathbf{B}$ plasma drifts in the equatorial ionosphere. In this paper, we focus on estimating daytime zonal drifts at the 150 km (140–160 km) and *E* (100–110 km) regions using multibeam observations of 150 km and *E* region echoes made using the EAR and study the daytime zonal drifts covering all seasons not studied before from Kototabang. Zonal drifts in the 150 km and *E* regions are found to be westward and mostly below -80 m s^{-1} and -60 m s^{-1} , respectively. While the zonal drifts in the 150 km and *E* regions do not go hand in hand on a case-by-case basis, the seasonal mean drifts in the two height regions are found to be in good agreement with each other. Zonal drifts at the 150 km region show seasonal variations with three maxima peaking around May, September, and January. The zonal drifts at the 150 km region are found to be smaller than the *F* region drifts obtained from Coupled Ion Neutral Dynamics Investigation (CINDI) onboard Communication and Navigation Outage Forecasting System (C/NOFS) by about 25 m s^{-1} consistent with the height variations of *F* region zonal drifts observed by the Jicamarca radar. These results constitute the first comprehensive study of zonal drifts at the 150 km and *E* regions from Kototabang, Indonesia, and the results are discussed in the light of current understanding on the low-latitude electrodynamics and coupling.

1. Introduction

Quiet time ionospheric $\mathbf{E} \times \mathbf{B}$ plasma drifts are driven primarily by the dynamo effects of thermospheric winds, which include the forcing from the lower atmospheric waves [e.g., Richmond, 1995; Heelis, 2004; Maute et al., 2012; Liu et al., 2013]. In the equatorial ionosphere, both zonal and vertical electric fields play important role in the electrodynamics and plasma instability processes. Most of the measurements on electric fields/plasma drifts available in the literature correspond to the *F* region, and these measurements have been made either by the Jicamarca incoherent scatter radar [Woodman, 1970; Fejer, 1997, 2011] or by satellite borne sensors [Fejer et al., 2008, 2013; Kil et al., 2009; Stoneback et al., 2011; Coley et al., 2014]. *E* region electric fields have also been measured. They have been estimated using the Doppler shifts of the *E* region type-II echoes observed by the coherent backscattered radars [e.g., Balsley, 1973; Reddy et al., 1987; Denardini et al., 2013; Moro et al., 2016]. While satellite-borne measurements have provided important information on the global-scale variations of both zonal and vertical electric fields, temporal variations of electric field have only been revealed using ground-based radar techniques. Zonal drifts at the *F* region have also been estimated using spaced scintillation receivers and airglow imaging techniques during the occurrence of plasma bubble and scintillation [e.g., Vacchione et al., 1987; Valladares et al., 1996; Bhattacharyya et al., 2001; Pimenta et al., 2003; Chapagain et al., 2011; Taori and Sindhya, 2014]. These measurements, however, are confined to nighttime and importantly have height uncertainty. Observations showed that *F* region plasma usually drifts westward and upward during the day and eastward and downward during the night. These drifts also show remarkable local time, seasonal and solar activity dependence [Fejer et al., 1991, 2005].

The daytime electric fields are primarily generated by the dynamo action of the *E* region, and the height profile of the electric field is thus governed by the latitudinal variation of electric field [Fejer et al., 2008]. Local time variations of these drifts, however, have so far been confined to Jicamarca sector due to lack of incoherent scatter radar in other longitudes. In the recent past, however, it has been shown that the vertical Doppler

Table 1. Month Wise Distribution of Number of Days of Observations and Number of Days on Which 150 km Echoes Were Observed

| Month | Number of Days of Observation | Number of Days of Observations on Which 150 km Echo Were Observed |
|-----------|-------------------------------|---|
| January | 8 | 6 |
| February | 1 | 1 |
| March | 6 | 0 |
| April | 15 | 3 |
| May | 20 | 8 |
| June | 20 | 12 |
| July | 26 | 12 |
| August | 14 | 9 |
| September | 14 | 11 |
| October | 9 | 4 |
| November | 10 | 5 |
| December | 23 | 18 |

shift of the 150 km echoes could be used as reliable means to measure daytime F region vertical $\mathbf{E} \times \mathbf{B}$ drift [Kudeki and Fawcett, 1993; Chau and Woodman, 2004], which opened up the use of these echoes for studying the daytime electrodynamics [Chau *et al.*, 2009; Alken, 2009].

Following the successful applications of the daytime 150 km echoes in estimating zonal electric field, Patra *et al.* [2012, 2014] have used the mesosphere-stratosphere-troposphere (MST) radar located at Gadanki, India, and the Equatorial Atmosphere Radar (EAR) located at Kototabang,

Indonesia, to study vertical $\mathbf{E} \times \mathbf{B}$ drift in the Indian and Indonesian sectors. These drifts have further been used to study the role of vertical $\mathbf{E} \times \mathbf{B}$ drift on the formation of the F_3 layer and $\mathbf{E} \times \mathbf{B}$ drift variations in the Indian sector linked with the major sudden stratospheric warming of 2009 [Pavan Chaitanya *et al.*, 2013; Patra *et al.*, 2014]. Vertical $\mathbf{E} \times \mathbf{B}$ drift has also been studied using the 150 km echoes from Brazil [Rodrigues *et al.*, 2013, 2015]. Daytime zonal plasma drifts in the 150 km region, however, are still unknown in these longitude sectors.

Given the fact that Doppler shifts of the 150 km echoes are governed by electric field (due to insignificant neutral-ion collision frequency), these echoes could be used to study zonal drift in the 140–170 km region, which is not accessible by satellite. Thus, the 150 km echoes could provide additional new data set on zonal drift in the F_1 region, which will help link the forcing from the E region below to the F region above. Also, the fact that the off-electrojet low-latitude 150 km region is connected to the equatorial F region via the magnetic field lines, zonal drifts derived using the 150 km echoes could be used for studying the F region electrodynamics over the magnetic equator and the E - F region coupling via magnetic field lines.

In this paper, we study zonal $\mathbf{E} \times \mathbf{B}$ drifts in the 150 km region estimated using multibeam observations of the daytime 150 km echoes made by the EAR from Kototabang (0.2°S, 100.32°E, 10.36°S magnetic latitude), Indonesia. We also use the simultaneously observed E region type-II echoes in the height range of 100–110 km by the same radar to make a comparative study of the zonal drifts of the irregularities at 150 km and 100–110 km regions. We also compare the zonal drifts at 150 km with those of the F region measured by the Coupled Ion Neutral Dynamics Investigation (CINDI) on board the C/NOFS [Coley *et al.*, 2014]. These results are first of its kind from Kototabang, Indonesia, and provide important information on the off-electrojet low-latitude electrodynamics in the E and F_1 regions during daytime, not studied before from Kototabang.

2. EAR Observations and Drift Estimation

Radar observations of zonal drifts in the 150 km and E regions presented in this paper were made using the 47 MHz Equatorial Atmosphere Radar (EAR) located at Kototabang [Fukao *et al.*, 2003]. These drifts have been estimated using the daytime 150 km and E region type-II echoes [Patra *et al.*, 2008; Yokoyama *et al.*, 2009]. Observations were made on 166 days spread over 2008–2010, when solar activity was minimum with $F_{10.7}$ of 60–76 solar flux units and daytime 150 km echoes were observed on 89 days. On these days, geomagnetic activities were quite with Kp values <3 . Month wise distribution of EAR observations used in this study is listed in Table 1. Accordingly, results presented in this paper are based on the 89 days of observations.

Observations were made using three beams: (Beam 1: azimuth 165°, zenith 21.84°), (Beam 2: azimuth 180°, zenith 21.23°), and (Beam 3: azimuth 195°, zenith 21.98°), which satisfy perpendicularity to Earth's magnetic field to detect the echoes from the E and 150 km region field-aligned irregularities. Other important radar parameters used in the observations were the following: pulse width 64 μ s with complementary code of 8 μ s baud length, interpulse period 1.6 ms, number of coherent integration 14, number of FFT points 256,

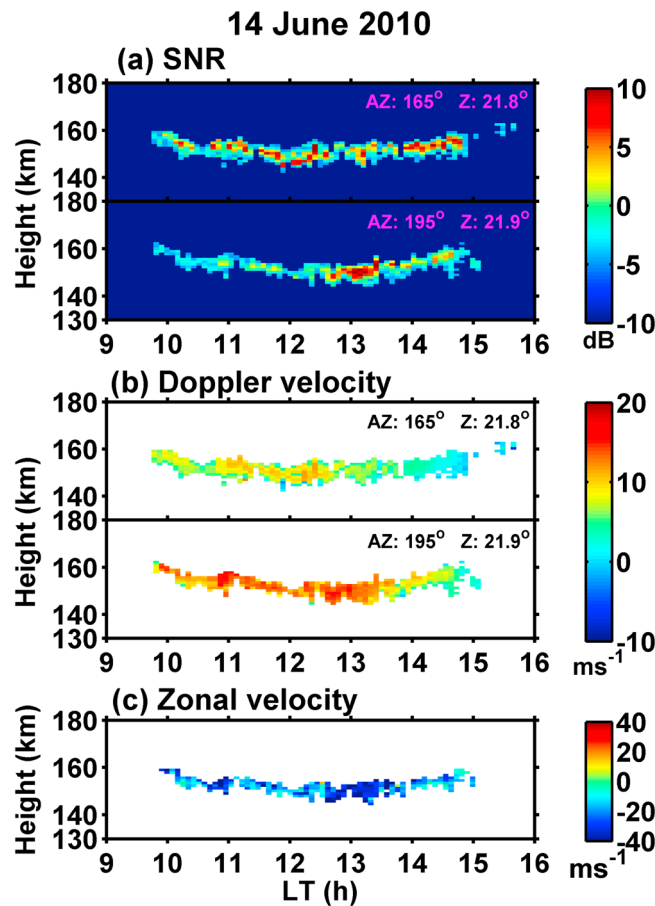


Figure 1. Height-time variations of (a) SNR and (b) radial Doppler velocity observed in Beam 1 (azimuth—165°) and Beam 3 (azimuth—195°) and (c) zonal velocity observed on 14 June 2010. In Figure 1c, positive (negative) values represent eastward (westward) velocities.

between Beam 1/Beam 3 and Beam 2 on the plane perpendicular to the geomagnetic field. More details on similar observations and zonal drift estimation can be found in Yokoyama *et al.* [2009].

3. Observational Results

3.1. Zonal Drifts at the 150 km Region

Figure 1a shows SNR of 150 km echoes observed on 14 June 2010 using Beam 1 and Beam 3. It may be noted that while the morphology of the echoes observed by both beams shows similar forenoon descent and afternoon ascent, echoes observed by Beam 1 are stronger than those of Beam 3, which is very similar to that reported earlier by Yokoyama *et al.* [2009]. Corresponding radial velocities, which represent $-\lambda/2$ (≈ 3.2 m) times the mean Doppler shifts, are shown in Figure 1b. Doppler velocities observed in Beam 3 are higher than those of Beam 1 indicating that the zonal drifts of the irregularities are westward. Figure 1c presents height-time variations of zonal drift (V_{zonal}) estimated following the method mentioned in section 2. Positive (negative) values of V_{zonal} represent eastward (westward) drifts. Note that zonal drifts in the 150 km region are westward and vary in the range of -10 to -40 m s^{-1} . At times, the drifts are as high as -80 m s^{-1} . However, no noticeable height variation in zonal drift is found.

Figures 2a–2c illustrate day-to-day variations of zonal drift based on observations made on a few days in June 2010, December 2009, and September 2008. Given that 150 km echoes do not occur regularly and also do not occur during the entire day, these observations have been chosen for demonstration since the 150 km echoes were observed on 6 or more consecutive days in these months. These represent zonal drift

and number of spectral averaging 10. These observations were conducted in such a way that the primary objectives of the EAR to study winds, waves, and turbulence in the troposphere and lower stratosphere were not compromised. Accordingly, we obtained spectral data for the range of 90–219.6 km with a range resolution of 1.2 km, unambiguous velocity of ± 71.2 m s^{-1} , and velocity resolution of 0.56 m s^{-1} . The time resolution between two sets of three-beam measurements was 343 s.

For the present study, we have used radar observations of the daytime 150 km echoes and *E* region type-II echoes made using Beam 1 and Beam 3. Zonal velocities of the irregularities, obtained from the Doppler shifts of these echoes, have been derived as follows:

$$V_{\text{zonal}} = (V_1 - V_2) / 2 \sin \theta, \quad (1)$$

where V_{zonal} is the zonal velocity of the irregularities, V_1 and V_2 are the radial Doppler velocities observed in Beam 1 (azimuth 165°) and Beam 3 (azimuth 195°), respectively, and θ ($\approx 5.4^\circ$) is the angle

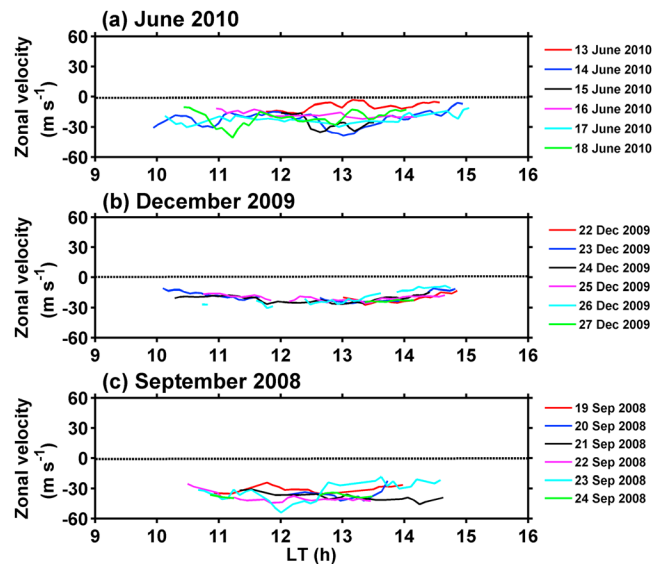


Figure 2. Day-to-day variations of zonal velocity at ~ 150 km in (a) June 2010, (b) December 2009, and (c) September 2008. These represent zonal velocity averaged over the height region of 140–165 km.

[Fejer *et al.*, 1991, 2005] and C/NOFS [Fejer *et al.*, 2013]. Later, we will make a one-to-one comparison between the zonal drifts at 150 km observed by the EAR and the *F* region drifts observed by CINDI onboard C/NOFS.

Since the height of occurrence of 150 km echoes varies on a day-to-day basis, it is quite likely that the day-to-day variation of zonal drift could be due to height variation of the echoes. In order to verify this possibility, we have examined the height-time variations of zonal drifts corresponding to the data shown in Figure 2 and the

averaged over height. Zonal drifts are all westward representing the governance of upward electric field during daytime, and the zonal drifts are confined to -50 m s^{-1} . Note that while there is noticeable day-to-day variations in June and September data, variations are very little in December. Nevertheless, these drifts are similar to those reported earlier using limited observations of 150 km echoes made by the EAR [Yokoyama *et al.*, 2009] and by the Jicamarca radar [Chau and Woodman, 2004] and more recently using an extensive data set of the Jicamarca radar [Hui and Fejer, 2015]. These drifts also appear to be broadly similar to those of daytime average *F* region drifts reported using the Jicamarca incoherent scatter radar

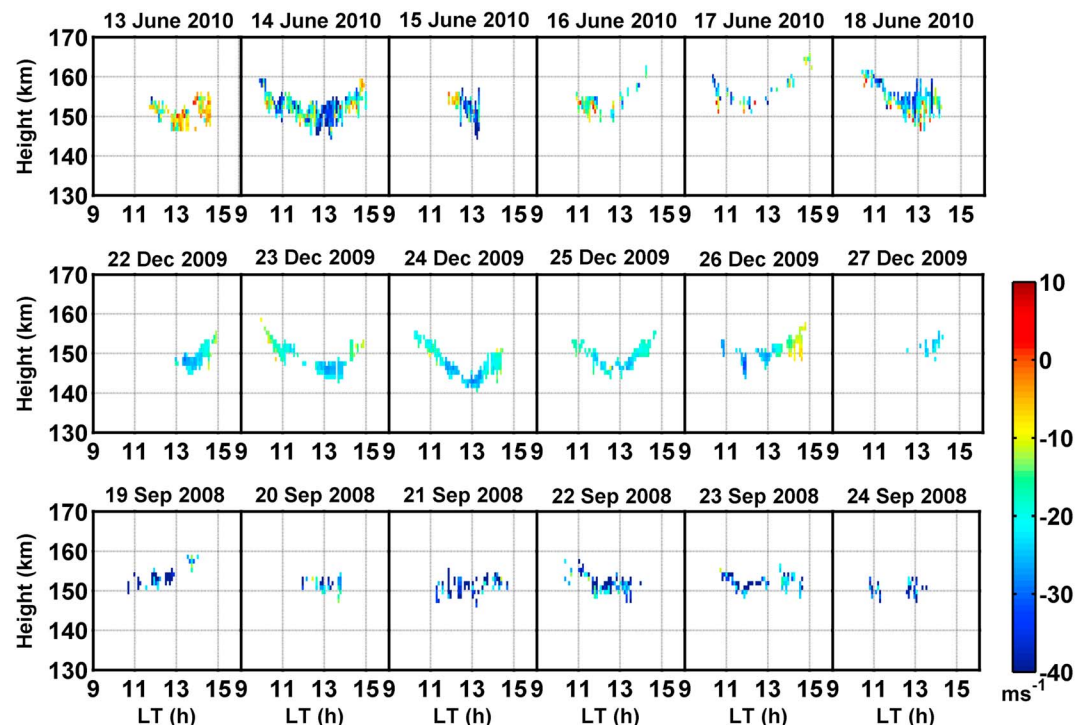


Figure 3. Height-time variations of zonal velocity on a day-to-day basis in (top row) June 2010, (middle row) December 2009, and (bottom row) September 2008. Positive (negative) values represent eastward (westward) velocities.

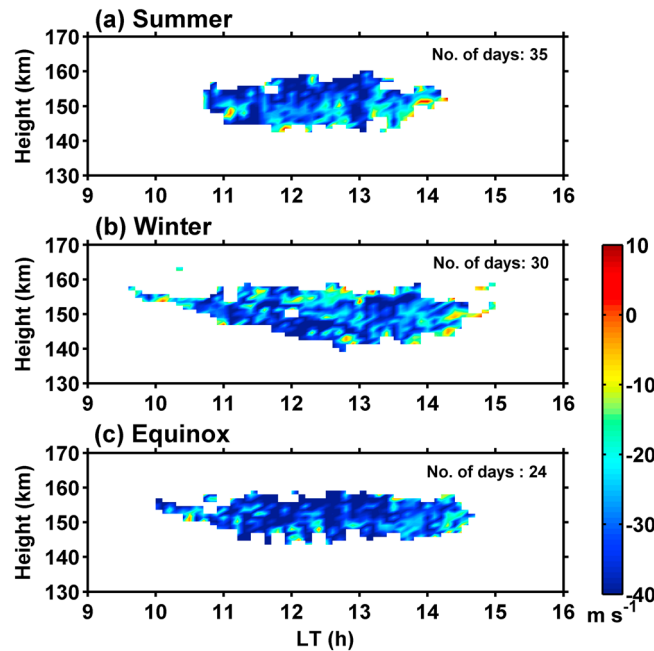


Figure 4. Height-time variations of mean zonal velocity observed in (a) summer (May–August), (b) winter (November–February), and (c) equinoxes (September–October and March–April). Negative values represent westward velocities.

winter (November–February), and equinox (September–October and March–April) in Figures 4a–4c, respectively. Number of days of observations used in estimating seasonal mean drifts are 35, 30, and 24 days corresponding to summer, winter, and equinox, respectively. The mean drifts are in the range of -15 to -40 m s^{-1} and are found not to vary much with season. Also, in the height region of 140–160 km, we do not find any noticeable increasing or decreasing pattern in the zonal drift.

Considering that the zonal drifts in the height region of 140–160 km do not vary much with height, we have studied their monthly variations. Figure 5a illustrates monthly mean along with standard deviation of zonal drifts at different local time periods (11–12 LT, 12–13 LT, and 13–14 LT) in different colors, and Figure 5b represents month wise distribution of data points used for the monthly mean zonal drifts. These represent

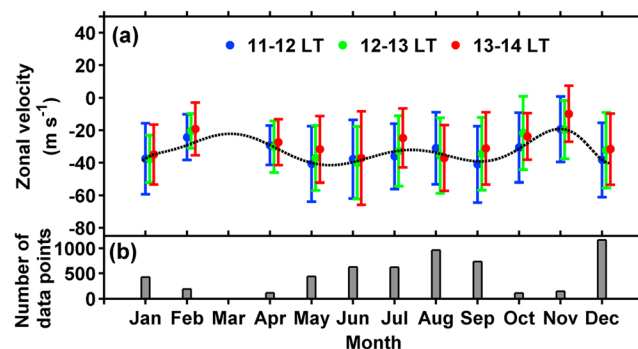


Figure 5. Monthly mean and standard deviation of zonal drifts observed corresponding to local time periods of 11–12 LT (blue), 12–13 LT (green), and 13–14 LT (red). Vertical bars represent standard deviations. Seasonal variation is shown by the best fit line shown in black. (b) Number of data points used in deriving monthly mean velocity.

results are illustrated in Figure 3. Figures 3 (top row), 3 (middle row), and 3 (bottom row) illustrate height-time variations of zonal drift observed during June, December, and September, respectively. It may be noted that the 150 km echoes are mostly confined to the altitude range of 145–160 km, and the day-to-day variation in the height of echo occurrence is small. These figures clearly suggest that while there is some variations of zonal drift with height, the day-to-day variations of zonal drift are primarily due to day-to-day variations in the drift itself. For example, zonal drifts observed on 13 and 16 June are clearly different from those observed on the rest of the days in June.

In order to examine whether there exists any height gradient in the zonal drifts in the height range of 140–160 km, we have plotted mean seasonal drifts as a function of height and time for summer (May–August), winter (November–February), and equinox (September–October and March–April) in Figures 4a–4c, respectively. The monthly mean drifts are limited to -40 m s^{-1} with standard deviation of 20 m s^{-1} . This implies that the drifts could often reach -60 m s^{-1} . This figure further suggests that zonal drifts at 150 km have three maxima occurring around May, September, and January. This figure also suggests the equinoctial asymmetry in zonal drift; i.e., the drifts are higher during the September equinox than during the March equinox. Considering that numbers of data point are limited during the two equinoxes, this asymmetry needs to be further examined

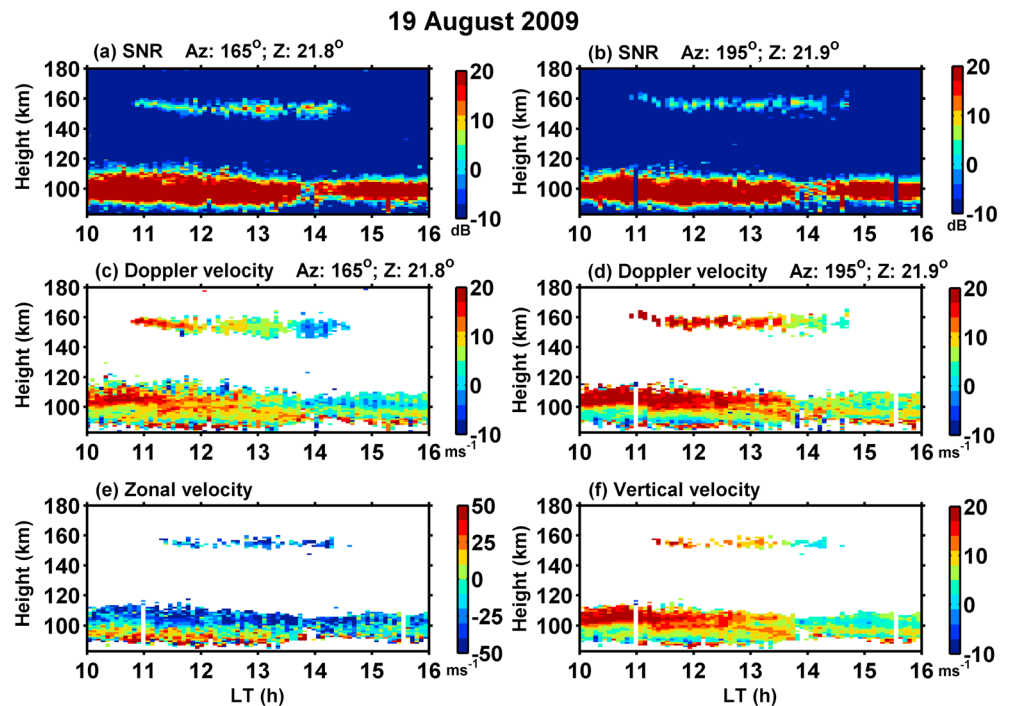


Figure 6. Height-time variations of 150 km and *E* region echo SNR observed on 19 August 2009 in (a) Beam 1 and (b) Beam 3. (c, d) Height-time variations of corresponding radial Doppler velocities. Height-time variations of (e) zonal velocity and (f) vertical velocity estimated using Beam 1 and Beam 3 observations.

with a larger database. It is quite likely that the observed seasonal variations, including equinoctial asymmetry, in the zonal drift are linked with variations in the tidal activity [Tsuda *et al.*, 1999]. Tsuda *et al.* [1999] investigated the tidal variability in the mesosphere/lower thermospheric wind over Jakarta, Indonesia, and found systematic seasonal variations. They also found substantial interannual variability in the tidal parameters. While we note that the seasonal variations in the zonal drifts reported here are quite similar to those reported by Tsuda *et al.* [1999], a detailed investigation based on concurrent observations of ionospheric drifts and neutral wind would be required to clarify the possible role of tides on the seasonal variations of zonal drifts.

3.2. Comparison of Zonal Drifts at the 150 km and *E* Regions

As mentioned earlier, the EAR observations can be used for estimating zonal drifts at the *E* region altitudes using the Doppler shift of the *E* region type-II echoes. At the upper part of the *E* region (typically >100 km), where the collision frequencies of electron and ion with neutral are significantly small, the Doppler shifts of the type-II echoes are predominantly governed by electric field [Reddy *et al.*, 1987]. Accordingly, the zonal drifts would represent vertical electric field. The drifts estimated using the type-II echoes have been derived in the same way as that of the 150 km drifts, which has been described in section 2. Figure 6 shows observations of 150 km and *E* region echoes observed on 19 August 2009. Figures 6a and 6b show height-time variations of signal-to-noise ratio (SNR) of the echoes observed by Beam 1 and Beam 3, respectively. Both 150 km and *E* region echoes occurred simultaneously and continuously for about 4 h (10:30–14:30 LT). Although such simultaneous occurrence of both 150 km and *E* region echoes is not regular, they occur quite frequently to make a comparative study of the drifts at the 150 km and *E* regions. Note that the *E* region echoes are at least 10 dB stronger than those of 150 km echoes. Again, the 150 km echoes observed by Beam 1 are somewhat stronger than those of Beam 3 consistent with that reported earlier by Yokoyama *et al.* [2009]. Radial velocities observed in these beams are shown in Figures 6c and 6d. Velocities of both 150 km and *E* region echoes observed in Beam 3 are more than those observed in Beam 1, indicating westward and upward/northward velocities of the echoes. Figures 6e and 6f show zonal and vertical drifts, respectively, estimated using the observations shown in Figures 6c and 6d. Strictly speaking, at Kototabang we measure drifts in the direction perpendicular to magnetic field in

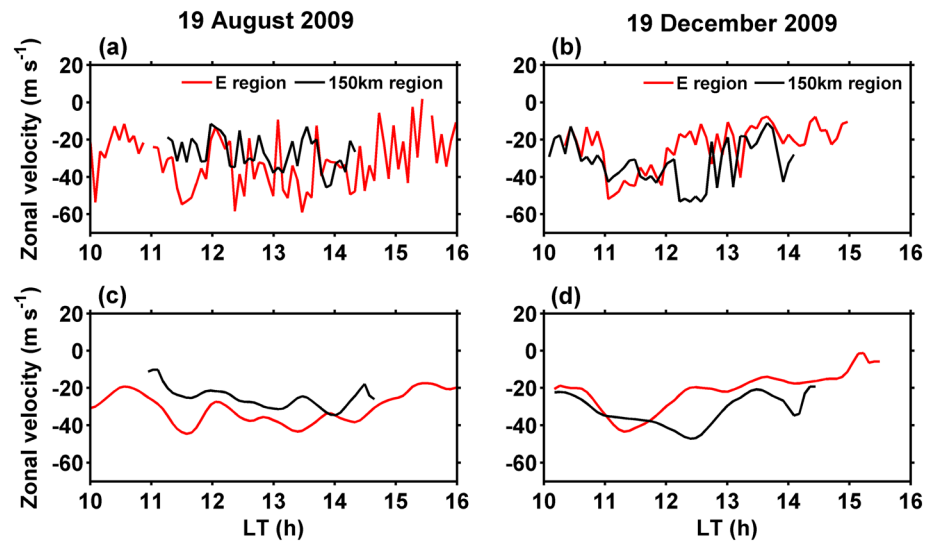


Figure 7. Temporal variations of zonal velocities at 150 km (black) and at *E* region above 100 km (red) averaged over height observed on (a) 19 August 2009 and (b) 19 December 2009. (c, d) Same as Figures 7a and 7b but after running average of 1 h.

the magnetic meridian plane, which is driven by zonal electric field. They are not vertical drifts, but for convenience and also for comparison with the dip equatorial vertical drifts, we consider them as vertical drifts. It may be noted from Figure 6e that the zonal drifts at 150 km and the upper part of the *E* regions (100–110 km) are westward with values mostly confined to -60 m s^{-1} . The drifts at the upper part of the *E* region, however, are higher than those of the 150 km region. Zonal drifts at altitudes below 100 km, however, are found to be eastward with values as high as 40 m s^{-1} . It is also interesting to note from Figure 6f that the vertical velocities are upward in the 150 km and upper part of *E* regions ($>100 \text{ km}$), and these drifts follow similar local time variations; i.e., the drifts in the early part of the observational run are more upward than those observed during the later time. Vertical drifts at altitudes below 100 km although are upward; they are smaller than those of altitudes $>100 \text{ km}$ and also 150 km region.

Figure 7 shows a detailed comparison of the zonal drifts estimated at 150 km and at altitudes of 100–110 km. For this purpose, we have considered the height-averaged drifts derived from the 150 km (140–160 km) echoes and the *E* region (100–110 km) type-II echoes. We have considered the zonal drifts of the *E* region type-II echoes in the altitude range of 100–110 km assuming that the drifts would be governed by electric field due to low values of collision frequency. Figures 7a and 7b show a comparison of height-averaged zonal drifts for the 150 km (black) and 100–110 km region (red) observed on 19 August and 19 December 2009, respectively. Both observations show considerable temporal variations with periods of 15–45 min, which are very similar to those reported earlier [Reddy and Devasia, 1976; Viswanathan *et al.*, 1993; Aveiro *et al.*, 2009; Pavan Chaitanya *et al.*, 2014]. Reddy and Devasia [1976] reported fluctuations in the east-west electron drifts with periods of 20–30 min based on their VHF radar measurements from Trivandrum, India, and also found that these fluctuations correlated well with those of the horizontal magnetic field fluctuations. Later, Viswanathan *et al.* [1993] reported 30–90 min variations in the simultaneous observations of the *E* and *F* region zonal electric fields from Trivandrum and attributed to gravity waves. Aveiro *et al.* [2009], using radar observations from Sao Luis, Brazil, found vertical electric field fluctuations with periods of 4–30 min and attributed their observations to gravity wave wind-driven electric field. Pavan Chaitanya *et al.* [2014], using Gadanki radar observations, found 4–100 min periodicity in the vertical drifts estimated using the 150 km echoes, which they attributed to gravity wave effects. Considering that the observations presented here were made during geomagnetically quiet conditions, the observed variations in the zonal drift are most likely associated with gravity wave-induced electric fields [Kato, 1973; Anandarao *et al.*, 1977]. It is apparent that while the drifts at the two regions are westward, they do not agree on a one-to-one basis. To make a comparison of the background drifts, we have performed a 12 point running average (which is equivalent to 1 h) to smooth out the fluctuations. The comparisons are shown in Figures 7c and 7d corresponding to the data shown in

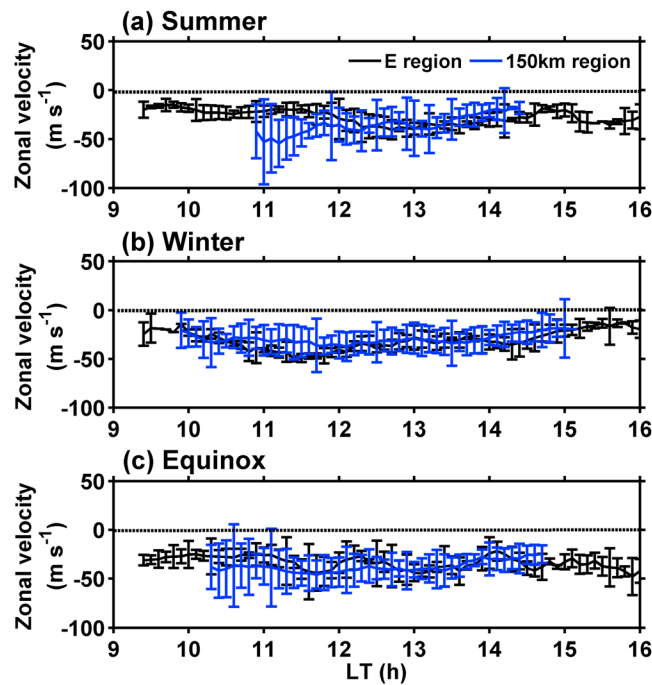


Figure 8. Local time variations of average zonal drift velocity and associated standard deviations in (a) summer, (b) winter, and (c) equinox. Blue and black lines in each panel represent the zonal drift at 150 km and the *E* regions (100–110 km), respectively.

ability than that of the *E* region. In this context, it may be mentioned that the average drifts in the 150 km and *E* regions have been derived using all available 150 km echoes and *E* region type-II echoes, respectively. Given the fact that echoes did not occur simultaneously on all the days, it is possible that the differences observed are partly biased by the occurrence pattern of the echoes in the two regions.

3.3. Comparison of Zonal Drifts at 150 km and *F* Regions

In order to examine whether the zonal drifts at 150 km over Kototabang agree with the equatorial *F* region drifts, we have examined concurrent observations of zonal drift made using the CINDI on board the C/NOFS.

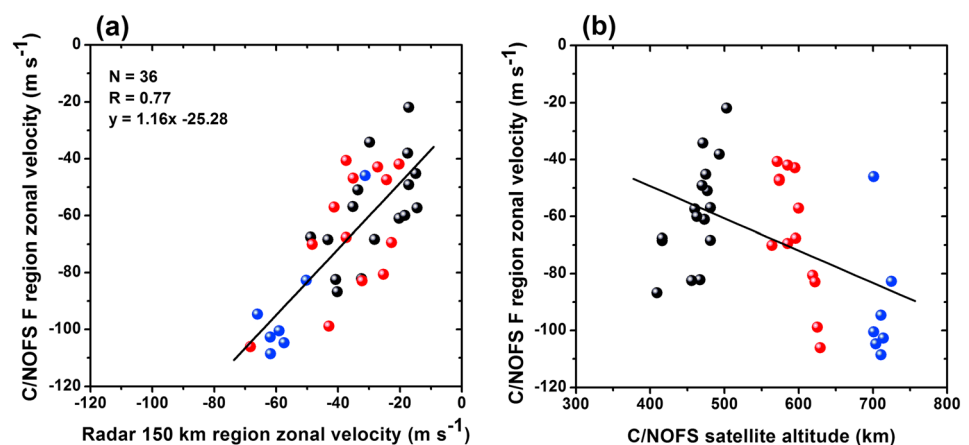


Figure 9. (a) Scatterplot of zonal drifts at the 150 km region estimated using the EAR observations and at the *F* region observed by the CINDI on board the C/NOFS. *N* and *R* represent the number of data points and correlation coefficient, respectively. Data shown in black, red, and blue colors correspond to different height regions, shown in Figure 9b. The best fit line is shown in black color. (b) Scatterplot of *F* region zonal velocity and corresponding height of the CINDI measurements along with the best fit line indicating the increasing zonal drift with increasing height.

Figures 7a and 7b, respectively. These figures clearly show that while the drifts are westward, the *E* region velocities are higher (lower) than those of the 150 km region on 19 August (19 December). Examination of simultaneous observations made on a few more days also reveals similar results.

Figures 8a–8c show comparisons of height-averaged drifts at 150 km (blue) and *E* region (black) during summer, winter, and equinoxes, respectively. The vertical bars represent standard deviations of these drifts. These figures clearly suggest that the mean zonal drifts at 150 km and *E* regions are broadly similar except for summer when the drifts at 150 km are higher than those of the *E* region especially around 11 LT. The larger standard deviations of the zonal drifts at 150 km than those of the *E* region, however, clearly suggest that zonal drift at 150 km has a larger day-to-day variability than that of the *E* region.

In this context, it may be mentioned that 150 km region over Kototabang connects the peak *F* region (~ 350 km) over the magnetic equator. For this purpose, we have used C/NOFS observations made on 36 days when the C/NOFS was within the longitude belt of $\pm 1^\circ$ centered on the EAR longitude (100.2°E) and $\pm 10^\circ$ centering on the magnetic equator. These observations were made during 2009–2010. Figure 9a shows scatter-plot of zonal drifts estimated from 150 km echoes and the *F* region drifts observed by the CINDI. Since the satellite altitude varied, we have used different colors for differentiating drifts measured in different height regions. Drifts presented in black, red, and blue correspond to the altitude regions of 400–500 km, 550–650 km, and 650–750 km, respectively. In Figure 9b, we also show how the drifts measured by the CINDI vary with height. From Figure 9a, we note that while both observations show westward drifts, *F* region drifts observed by the CINDI are clearly higher than those of the 150 km region observed by the EAR. The linear best fit curve indicates that on average the *F* region drifts are about 25 m s^{-1} higher than those of the 150 km region. On the other hand Figure 9b suggests that while zonal drift generally shows increasing trend with height, there also exists large day-to-day variation (which include local time and latitudinal variations). It is also important to mention that during the period of observations (2009–2010), solar activity was very low and ionospheric density was also very low, especially at altitudes above 500 km. Accordingly, the CINDI observations corresponding to altitudes above 500 km should be used with caution. Nevertheless, the increasing velocity with increasing height noted in Figure 9b is found to be broadly consistent with that reported based on Jicamarca radar observations [Hui and Fejer, 2015].

4. Summary and Discussion

Results on daytime zonal plasma drifts over Kototabang, Indonesia, presented in section 3 can be summarized as follows:

1. Daytime zonal drifts at the 150 km region are westward with values less than -80 m s^{-1} . The seasonal mean drifts are limited to -40 m s^{-1} and do not show any noticeable height variations in the height region of 140–160 km. Zonal drifts show seasonal variations with three maxima peaking around May, September, and January.
2. Daytime zonal drifts at the *E* region altitudes of 100–110 km are westward with mean velocities confined to -40 m s^{-1} .
3. Daytime zonal drifts at the 150 km and *E* regions generally do not agree to each other on a one-to-one basis, but their seasonal mean is quite comparable. Day-to-day variations, however, are found to be more at the 150 km region than that of the *E* region.
4. Daytime zonal drifts at 150 km region are lower than those of the *F* region by $\sim 25 \text{ m s}^{-1}$.

It may be mentioned that these results constitute the first comprehensive study of zonal drifts at the 150 km (140–160 km) and *E* region (100–110 km) from Kototabang, Indonesia. As for the zonal drifts at 150 km region, they are very similar to those reported by Chau and Woodman [2004] and Hui and Fejer [2015]. The seasonal average zonal drifts at the 150 km region are also broadly similar to the *F* region zonal drifts reported using Jicamarca incoherent scatter radar by Fejer *et al.* [2005]. This similarity may be partly due to averaging of drifts over the height region of 300–500 km performed by Fejer *et al.* [2005] and partly due to lower zonal drift in the Jicamarca sector than the rest of the globe as revealed by Fejer *et al.* [2013] using C/NOFS data. A detailed analysis on the height variation of daytime zonal drift [Hui and Fejer, 2015] clearly demonstrates that the drifts at 150 km are lower than those of the higher altitudes at any time of the day. In fact, Chau and Woodman [2004] using 150 km echoes and incoherent scatter measurements made using the Jicamarca radar showed that the *F* region drifts are higher than those of the 150 km region. Comparison of zonal drifts at the 150 km region with those of CINDI reported here has also clearly shown that the *F* region zonal drifts are higher than those of the 150 km region, and this difference is partly due to height variation of zonal drift consistent with that reported by Hui and Fejer [2015].

It may be important to mention here that the comparison of drifts between the 150 km region and *F* region performed here is special since these two regions are connected by the magnetic field lines, not just the height difference. We, however, have found that the drifts at the two regions are not similar; instead, the drifts at the *F* region are higher than those of the 150 km region, which is very similar to that reported by Hui and Fejer [2015] using the Jicamarca radar. Comparison of vertical drifts at the 150 km and *F* regions done earlier, however, showed a very good agreement between the two [Patra *et al.*, 2014].

Thus, the comparison of zonal drifts presented here implies that although the low-latitude 150 km region is connected to the dip equatorial F region by magnetic field lines, the vertical electric fields in the two height regions are different. It is quite likely that the 150 km region being close to the low-latitude E region and well coupled via the Earth's magnetic field lines, the vertical electric field in the 150 km region is controlled by the neutral winds in the E region. Chau and Woodman [2004] discussed the relationship among the vertical plasma drift, zonal plasma drift, and zonal neutral velocity and showed that these three parameters are related through the following equation:

$$V_x \approx - \left(\sum_H / \sum_P \right) V_z + \int (\sigma_P \times U_n ds) / \sum_P, \quad (2)$$

where σ_P is the Pedersen conductivity, \sum_H and \sum_P are the field line-integrated Hall and Pedersen conductivities, U_n is the neutral wind, and ds is the distance along the magnetic field line. Thus, the second term in equation (2) represents field line integral of the quantities in the parenthesis. Given the fact that the vertical drifts in the 150 km region and F region are similar [Patra et al., 2014], the difference in the zonal drifts in the two height regions can be attributed to the zonal neutral velocity. We, however, have found that the zonal drifts vary more at the 150 km region than that at the E region, implying that the coupling between the E and 150 km regions is quite involved and needs a detailed investigation.

5. Conclusions

We have performed a comprehensive study of daytime zonal drifts at the 150 km region and E region (>100 km) using the EAR observations from Kototabang, Indonesia. We have also made a detailed comparison of these drifts with those concurrently measured using the C/NOFS and those reported from Jicamarca for the 150 km and F regions. Results clearly show height variation in zonal drift in the F region but not so much height variation between the E region and 150 km. These results are the first of their kind from Kototabang, Indonesia, and are expected to help understand the electrodynamics and coupling processes.

Acknowledgments

The EAR project is partially supported by Grant-in-Aid for Scientific Research on Priority Area-764 of the Ministry of Education, Culture, Sports, Science and Technology of Japan. The operation of the EAR is based upon the agreement between RISH and LAPAN. Y.O. was supported by JSPS KAKENHI Grant 15H05815. P.P.C. gratefully acknowledges NARL for supporting his research. Data used in this work are available with A.K. Patra (akpatra@narl.gov.in) and can be availed upon request.

References

- Alken, P. (2009), A quiet time empirical model of equatorial vertical plasma drift in the Peruvian sector based on 150 km echoes, *J. Geophys. Res.*, *114*, A02308, doi:10.1029/2008JA013751.
- Anandarao, B. G., R. Raghavarao, and C. R. Reddy (1977), Electric fields by gravity wave winds in the equatorial ionosphere, *J. Geophys. Res.*, *82*, 1510–1512.
- Aveiro, H. C., C. M. Denardini, and M. A. Abdu (2009), Climatology of gravity waves-induced electric fields in the equatorial E region, *J. Geophys. Res.*, *114*, A11308, doi:10.1029/2009JA014177.
- Balsley, B. B. (1973), Electric fields in the equatorial ionosphere: A review of techniques and measurements, *J. Atmos. Terr. Phys.*, *35*, 1035–1044.
- Bhattacharyya, A., S. Basu, K. M. Groves, C. E. Valladares, and R. Sheehan (2001), Dynamics of equatorial F region irregularities from spaced receiver scintillation observations, *Geophys. Res. Lett.*, *28*, 119–122.
- Chapagain, N. P., M. J. Taylor, and J. V. Eccles (2011), Airglow observations and modeling of F region depletion zonal velocities over Christmas Island, *J. Geophys. Res.*, *116*, A02301, doi:10.1029/2010JA015958.
- Chau, J. L., and R. F. Woodman (2004), Daytime vertical and zonal velocities from 150 km echoes: Their relevance to F region dynamics, *Geophys. Res. Lett.*, *31*, L17801, doi:10.1029/2004GL020800.
- Chau, J. L., B. G. Fejer, and L. P. Goncharenko (2009), Quiet variability of equatorial $E \times B$ drifts during a sudden stratospheric warming event, *Geophys. Res. Lett.*, *36*, L17801, doi:10.1029/2008GL036785.
- Coley, W. R., R. A. Stoneback, R. A. Heelis, and M. R. Hairston (2014), Topside equatorial zonal ion velocities measured by C/NOFS during rising solar activity, *Ann. Geophys.*, *32*(2), 69–75, doi:10.5194/angeo-32-69-2014.
- Denardini, C. M., H. C. Aveiro, J. H. A. Sobral, J. V. Bageston, L. M. Guizelli, L. C. A. Resende, and J. Moro (2013), E region electric fields at the dip equator and anomalous conductivity effects, *Adv. Space Res.*, *51*, 1857–1869.
- Fejer, B. G. (1997), The electrodynamics of the low-latitude ionosphere: Recent results and future challenges, *J. Atmos. Sol. Terr. Phys.*, *59*, 1456–1482, doi:10.1016/S1364-6826(96)00149-6.
- Fejer, B. G. (2011), Low latitude ionospheric electrodynamics, *Space Sci. Rev.*, *158*(1), 145–166, doi:10.1007/s11214-010-9690-7.
- Fejer, B. G., E. R. de Paula, S. A. Gonzalez, and R. F. Woodman (1991), Average vertical and zonal F region plasma drifts over Jicamarca, *J. Geophys. Res.*, *96*(A8), 13,901–13,906, doi:10.1029/91A01171.
- Fejer, B. G., J. R. Souza, A. S. Santos, and A. E. C. Perreira (2005), Climatology of F region zonal drifts over Jicamarca, *J. Geophys. Res.*, *110*, A12310, doi:10.1029/2005JA011324.
- Fejer, B. G., J. W. Jensen, and S.-Y. Su (2008), Quiet time equatorial F region vertical plasma drift model derived from ROCSAT-1 observations, *J. Geophys. Res.*, *113*, A05354, doi:10.1029/2007JA012801.
- Fejer, B. G., B. D. Tracy, and R. F. Pfaff (2013), Equatorial zonal plasma drifts measured by the C/NOFS satellite during the 2008–2011 solar minimum, *J. Geophys. Res. Space Physics*, *118*, 3891–3897, doi:10.1002/jgra.50382.

- Fukao, S., H. Hashiguchi, M. Yamamoto, T. Tsuda, T. Nakamura, M. K. Yamamoto, T. Sato, M. Hagio, and Y. Yabugaki (2003), Equatorial Atmospheric Radar (EAR): System description and first results, *Radio Sci.*, *38*(3), 1053, doi:10.1029/2002RS002767.
- Heelis, R. A. (2004), Electrodynamics in the low and middle latitude ionosphere: A tutorial, *J. Atmos. Sol. Terr. Phys.*, *66*(10), 825–838, doi:10.1016/j.jastp.2004.01.034.
- Hui, D., and B. G. Fejer (2015), Daytime plasma drifts in the equatorial lower ionosphere, *J. Geophys. Res. Space Physics*, *120*, 9738–9747, doi:10.1002/2015JA021838.
- Kato, S. (1973), Electric field and wind motion at the magnetic equator, *J. Geophys. Res.*, *78*, 757–762.
- Kil, H., S.-J. Oh, L. J. Paxton, and T.-W. Fang (2009), High-resolution vertical $E \times B$ drift model derived from ROCSAT-1 data, *J. Geophys. Res.*, *114*, A10314, doi:10.1029/2009JA014324.
- Kudeki, E., and C. D. Fawcett (1993), High resolution observations of 150 km echoes at Jicamarca, *Geophys. Res. Lett.*, *20*, 1987–1990.
- Liu, H.-L., V. A. Yudin, and R. G. Roble (2013), Day-to-day ionospheric variability due to lower atmosphere perturbations, *Geophys. Res. Lett.*, *40*, 665–670, doi:10.1002/grl.50125.
- Maute, A., A. D. Richmond, and R. G. Roble (2012), Sources of low-latitude ionospheric $E \times B$ drifts and their variability, *J. Geophys. Res.*, *117*, A06312, doi:10.1029/2011JA017502.
- Moro, J., C. M. Denardini, L. C. A. Resende, S. S. Chen, and N. J. Schuch (2016), Equatorial E region electric fields at the dip equator: 1. Variabilities in eastern Brazil and Peru, *J. Geophys. Res. Space Physics*, *121*, 10,220–10,230, doi:10.1002/2016JA022751.
- Patra, A. K., T. Yokoyama, Y. Otsuka, and M. Yamamoto (2008), Daytime 150-km echoes observed with the Equatorial Atmosphere Radar in Indonesia: First results, *Geophys. Res. Lett.*, *35*, L06101, doi:10.1029/2007GL033130.
- Patra, A. K., P. P. Chaitanya, N. Mizutani, Y. Otsuka, T. Yokoyama, and M. Yamamoto (2012), A comparative study of equatorial daytime vertical $E \times B$ drift in the Indian and Indonesian sectors based on 150 km echoes, *J. Geophys. Res.*, *117*, A11312, doi:10.1029/2012JA018053.
- Patra, A. K., P. P. Chaitanya, Y. Otsuka, T. Yokoyama, M. Yamamoto, R. A. Stoneback, and R. A. Heelis (2014), Vertical $E \times B$ drifts from radar and C/NOFS observations in the Indian and Indonesian sectors: Consistency of observations and model, *J. Geophys. Res. Space Physics*, *119*, 3777–3788, doi:10.1002/2013JA019732.
- Pavan Chaitanya, P., A. K. Patra, N. Balan, and S. V. B. Rao (2013), First simultaneous observations of F_3 layer and $E \times B$ drift in Indian sector and modeling, *J. Geophys. Res. Space Physics*, *118*, 3527–3539, doi:10.1002/jgra.50298.
- Pavan Chaitanya, P., A. K. Patra, and S. V. B. Rao (2014), Quiet time short-period and day-to-day variations in $E \times B$ drift studied using 150 km radar echoes from Gadanki, *J. Geophys. Res. Space Physics*, *119*, 3053–3065, doi:10.1002/2013JA019668.
- Pimenta, A. A., J. A. Bittencourt, Y. Sahai, R. A. Buriti, H. Takahashi, and M. J. Taylor (2003), Ionospheric plasma bubble zonal drifts over the tropical region: A study using OI (630.0 nm) emission all-sky images, *J. Atmos. Sol. Terr. Phys.*, *65*, 1117–1126, doi:10.1016/S1364-8626(03)00149-4.
- Reddy, C. A., and C. V. Devasia (1976), Short period fluctuations of the equatorial electrojet, *Nature*, *261*, 396–397.
- Reddy, C. A., B. T. Vikramkumar, and K. S. Viswanathan (1987), Electric fields and currents in the equatorial electrojet deduced from VHF radar observations—I. A method of estimating electric fields, *J. Atmos. Terr. Phys.*, *49*, 183–191.
- Richmond, A. D. (1995), Ionospheric electrodynamics, in *Handbook of Atmospheric Electrodynamics*, vol. 2, edited by H. Volland, pp. 249–290, CRC Press, Boca Raton, Fla.
- Rodrigues, F. S., E. B. Shume, E. R. de Paula, and M. Milla (2013), Equatorial 150 km echoes and daytime F region vertical plasma drifts in the Brazilian longitude sector, *Ann. Geophys.*, *31*(10), 1867–1876, doi:10.5194/angeo-31-1867-2013.
- Rodrigues, F. S., J. M. Smith, M. Milla, and R. A. Stoneback (2015), Daytime ionospheric equatorial vertical drifts during the 2008–2009 extreme solar minimum, *J. Geophys. Res. Space Physics*, *120*, 1452–1459, doi:10.1002/2014JA020478.
- Stoneback, R. A., R. A. Heelis, A. G. Burrell, W. R. Coley, B. G. Fejer, and E. Pacheco (2011), Observations of quiet time vertical drift in the equatorial ionosphere during the solar minimum period of 2009, *J. Geophys. Res.*, *116*, A12327, doi:10.1029/2011JA016712.
- Taori, A., and A. Sindhya (2014), Measurements of equatorial plasma depletion velocity using 630 nm airglow imaging over a low-latitude Indian station, *J. Geophys. Res. Space Physics*, *119*, 396–401, doi:10.1002/2013JA019465.
- Tsuda, T., K. Ohnishi, F. Isoda, T. Nakamura, R. A. Vincent, I. M. Reid, S. W. Harijono, T. Sribimawati, A. Nuryanto, and H. Wiryosumarto (1999), Coordinated radar observations of atmospheric diurnal tides in equatorial regions, *Earth Planets Space*, *51*, 579–592.
- Vacchione, J. D., S. J. Franke, and K. C. Yeh (1987), A new analysis technique for estimating zonal irregularity drifts and variability in the equatorial F -region using spaced receiver scintillation data, *Radio Sci.*, *22*, 745–756.
- Valladares, C. E., R. Sheehan, S. Basu, H. Kuenzler, and J. Espinoza (1996), The multi-instrumented studies of equatorial thermosphere aeronomy scintillation system: Climatology of zonal drifts, *J. Geophys. Res.*, *101*, 26,839–26,850.
- Viswanathan, K. S., R. Balachandran Nair, and P. B. Rao (1993), Simultaneous observations of E and F region electric field fluctuations at the magnetic equator, *J. Atmos. Terr. Phys.*, *55*, 185–192.
- Woodman, R. (1970), Vertical drift velocities and east-west electric fields at the magnetic equator, *J. Geophys. Res.*, *75*(31), 6249–6259, doi:10.1029/JA075i031p06249.
- Yokoyama, T., D. L. Hysell, A. K. Patra, Y. Otsuka, and M. Yamamoto (2009), Zonal asymmetry of daytime 150-km echoes observed by Equatorial Atmosphere Radar in Indonesia, *Ann. Geophys.*, *27*, 967–974, doi:10.5194/angeo-27-967-2009.